Journal of Molecular Catalysis A: Chemical 355 (2012) 85–95

Contents lists available at SciVerse ScienceDirect

Journal of Molecular Catalysis A: Chemical

journal homepage: www.elsevier.com/locate/molcata

Experimental, DFT and kinetic study of 1-octene metathesis with Hoveyda–Grubbs second generation precatalyst

Percy van der Gryp*, Sanette Marx, Hermanus C.M. Vosloo

Research Focus Area for Chemical Resource Beneficiation, North-West University, Hoffman Street, Potchefstroom 2522, South Africa

ARTICLE INFO

Article history:
Received 22 July 2011
Received in revised form 28 October 2011
Accepted 1 December 2011
Available online 10 December 2011

Keywords:
Hoveyda–Grubbs
1-Octene
Metathesis
Kinetic
DFT

ABSTRACT

In this study we report the catalytic performance, reaction engineering kinetics and elucidation of the reaction mechanism using density functional theory (DFT) for the metathesis reaction of 1-octene in the presence of the Hoveyda–Grubbs 2 [$RuCl_2$(=CH—o—$O_iPrC_6H_4$)(H_2IMes)] precatalyst. The study showed that reaction temperature (30–100 °C), 1-octene/precatalyst molar ratio (5000–14,000) and different solvents had a significant effect on the selectivity, activity and turnover number. Turnover numbers as high as 6448 were observed. Two main reactions were observed, namely: metathesis over the entire temperature range and isomerization above 50 °C. The observed experimental product-time distribution data for the complex parallel reaction system was fairly accurately described by four pseudo-first order reaction rates. The effects of temperature (Arrhenius Equation) and precatalyst concentration were incorporated in the observed rate constant. The primary observed activation energy was approximately 24 kcal mol^{-1}, which is in agreement with the DFT computational values for the proposed Hoveyda–Grubbs mechanism.

1. Introduction

Over the past two decades, alkene metathesis has established itself as an excellent approach to synthesize a wide variety of valuable molecules with different applications ranging from natural product synthesis, medicinal chemistry, macromolecular architecture, solid-phase chemistry and complex molecule synthesis [1–3]. This is mainly thanks to the well-defined ruthenium carbene complexes, such as the Grubbs-based precatalysts, that are commercially available. The first ruthenium carbene precatalyst was prepared in 1992 and a few years later the well known first generation Grubbs precatalyst was reported [4–7] with its remarkable activity and excellent tolerance for a variety of functional groups and moisture. Unfortunately, the precatalyst demonstrated relative short lifetime in the reaction medium. The more active and stable second generation Grubbs precatalyst based on N-heterocyclic carbenes was discovered shortly thereafter. These discoveries and challenges have ushered in a multitude of different precatalysts in existence today [8].

One particular interesting type of precatalyst reported simultaneously by the groups of Hoveyda and Blechert, commonly known as the "Hoveyda–Grubbs" precatalyst, showed improved activity, stability and especially longer lifetimes in the reaction medium [9–11]. Furthermore the Hoveyda–Grubbs based precatalysts demonstrated air-stability, ease of storage and handling, as well as excellent catalyst recovery and reuse with high activity and selectivity [8–12]. It is considered one of the best catalysts for cross metathesis and ring closing metathesis.

Both kinetic and theoretical investigations have been reported for metathesis systems [13–29]. These studies mainly use kinetics to elucidate and optimize catalyst design so as to synthesize that "best catalyst". However, detailed reactor kinetic investigations with comparison to a fundamental theoretical understanding still lack in the field of metathesis, especially for the Hoveyda–Grubbs based systems. In view of our [30–34] longstanding industrial interest of converting low value alkenes to higher value alkenes, such as the conversion of 1-octene to internal alkenes which can then be used as inter alia detergent alcohol feedstock in a downstream process, we decided to investigate the metathesis reaction of 1-octene with the Hoveyda–Grubbs second generation precatalyst (**HGr2**).

It is therefore the aim of this publication to characterize the catalytic performances of the metathesis reaction of 1-octene with precatalyst **HGr2** and furthermore to describe the metathesis system from a reaction engineering viewpoint and to get a clearer understanding of the mechanism behind this system with a DFT-study.

* Corresponding author. Tel.: +27 18 299 1953; fax: +27 18 299 1667.
E-mail address: percy.vandergryp@nwu.ac.za (P. van der Gryp).

1381-1169/$ – see front matter © 2011 Elsevier B.V. All rights reserved.
doi:10.1016/j.molcata.2011.12.001

2. Experimental

2.1. Materials

The chemicals used for the self-metathesis reaction were 98% 1-octene (Aldrich) and the ruthenium carbene complex $RuCl_2(=CH{-}o{-}O_iPrC_6H_4)(H_2IMes)$ (Hoveyda–Grubbs second generation (**HGr2**), Aldrich). For GC analysis 99.8% toluene (Rochelle), 99% nonane (Aldrich) and tert-butyl hydroperoxide solution (Fluka) were used. All the chemicals were used as supplied without further purification.

2.2. Metathesis of 1-octene

The self-metathesis reactions of 1-octene were carried out in a 250 mL three-necked round-bottomed flask fitted with a condenser, thermometer and septum as reported previously [32]. The 1-octene (20 mL) was transferred to the reaction flask and heated to the desired reaction temperature (ranging from 30 to 100 °C) using an oil bath on a controlled hotplate magnetic stirrer. Thereafter the precatalyst amount (ranging from 7 to 22 mg) was added to the flask and the reaction mixture was continuously stirred with a magnetic stirrer bar until the formation of the primary metathesis products was completed. Samples (0.3 mL) were withdrawn with a gastight syringe during the reaction at different time intervals and added to a solution of nonane (0.1 mL), toluene (0.3 mL) and 2 drops of tert-butyl hydrogen peroxide for analysis by GC/FID. Nonane was used as an external standard, toluene was used to increase sample volume and tert-butyl hydrogen peroxide was used as a quencher. An Agilent 6890 GC equipped with an Agilent 7683 auto-injector, HP-5 capillary column (30 m × 320 μm × 0.25 μm) and a FID was used for analysis. The GC analysis conditions were: inlet temperature 200 °C; N_2 carrier gas flow rate 94 mL/min; injection volume 0.2 mL (auto injection); split ratio 50:1; oven programming 60 °C for 5 min, 60–110 °C at 25 °C/min, 110 °C for 5 min, 110–290 °C at 25 °C/min, 290 °C for 5 min; FID detector temperature 300 °C; H_2 flow rate 40 mL/min and air flow rate 450 mL/min.

2.3. Computational method

In order to validate and gain a deeper insight into the mechanism of precatalyst **HGr2** for the metathesis of 1-octene, molecular modelling was used. All the computational results in this investigation were calculated by using the DMol^3 DFT (density functional theory) code as implemented in Accelrys Materials Studio® 4.2. DFT was used since it is a popular and versatile method for producing realistic geometries, relative energies and vibrational frequencies for transition metal compounds. Previous studies [32,35] also applied this method to Grubbs-type precatalysts. DMol^3 utilizes a basis set of numeric atomic functions, which are exact solutions to the Kohn–Sham equations for the atom. The Kohn–Sham equations are a set of eigenvalue equations within DFT. These basis sets are generally more complete than a comparable set of linearly independent Gaussian functions and have been demonstrated to have small basis set superposition errors. In this investigation a polarized split valence basis set, termed double numeric polarized (DNP) basis set has been used. All geometry optimizations employed highly efficient delocalized internal coordinates. The use of delocalized coordinates significantly reduces the number of geometry optimization iterations needed to optimize larger molecules, compared to the use of traditional Cartesian coordinates. The non-local generalised gradient approximation (GGA) functional by Perdew and Wang (PW91) was used for all geometry optimizations. The convergence criteria for these optimizations consisted of threshold values of 2×10^{-5} Ha, 0.004 Ha/Å and 0.005 Å for energy, gradient and displacement convergence, respectively, while a self-consistent field (SCF) density convergence threshold value of 1×10^{-5} Ha was specified. The GCA/PW91/DNP DFT calculations were carried out on a cluster with the following specifications: 52 CPU cluster (HP Proliant CP4000 Linux Beowulf with Procurve Gb/E Interconnect on computer nodes): 1 × Master node: HP DL385 – 2 × 2.8 MHz AMD Opteron 64, 2 GB RAM, 2 × 72 GB HDD, 12 × Computer nodes: HP DL145G2 – 2 × 2.8 MHz AMD Opteron 64, 2 GB RAM, 2 × 36 GB HDD, Operating system on computer nodes: Redhat Enterprise Linux 4 Cluster operating system: HPC CMU v3.0 cluster. The optimized geometries were also subjected to full frequency analyses at the same GGA/PW91/DNP level of theory to verify the nature of the stationary points. Equilibrium geometries were characterized by the absence of imaginary frequencies. Transition state (TS) geometries were obtained by transition state geometries optimizations on the GGA/PW91/DNP level of theory. This ensured the direct connection of transition states with the respective reactant and product geometries. The transition structure geometries that were subjected to vibrational analyses exhibited one imaginary frequency in the reaction coordinate. All results were mass balanced for the isolated system in the gas phase. The energy values that are given in the results are the electronic energies at 0 K and, therefore, only the electronic effects are considered in this investigation.

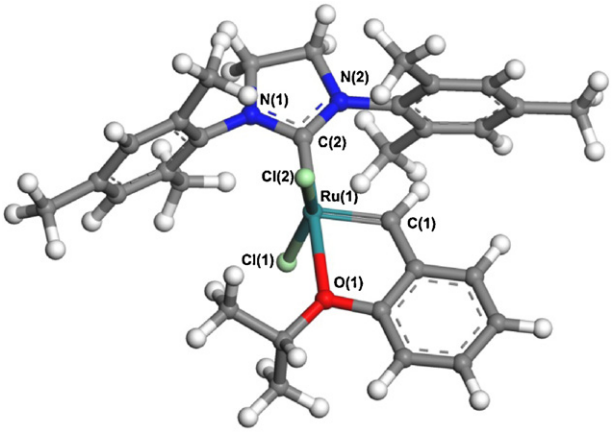

Fig. 1. Ball and stick presentation of DFT geometry optimized structure of precatalyst **HGr2**.

Table 1
DFT investigation and validation of computational method.

	Garber et al.[a]	DFT[b]	% Error
Bond lengths (Å)			
Ru(1)—C(1)	1.828(5)	1.871	2.352
Ru(1)—C(2)	1.981(5)	2.023	2.120
Ru(1)—O(1)	2.261(3)	2.352	4.025
Ru(1)—Cl(1)	2.328(12)	2.382	2.320
Ru(1)—Cl(2)	2.340(12)	2.383	1.838
C(2)—N(1)	1.351(6)	1.367	1.184
C(2)—N(2)	1.350(6)	1.360	0.741
Bond angles (°)			
C(1)—Ru(1)—O(1)	79.3(17)	77.675	2.049
C(1)—Ru(1)—C(2)	101.5(14)	102.050	0.542
C(2)—Ru(1)—O(1)	176.2(14)	178.898	1.531
C(1)—Ru(1)—Cl(1)	100.2(15)	100.35	0.150
C(1)—Ru(1)—Cl(2)	100.1(15)	98.474	1.624
O(1)—Ru(1)—Cl(1)	86.9(9)	86.229	0.772
O(1)—Ru(1)—Cl(2)	85.3(9)	85.064	0.277
C(2)—Ru(1)—Cl(1)	96.6(12)	96.034	0.586
C(2)—Ru(1)—Cl(2)	90.9(12)	92.779	2.067
Cl(1)—Ru(1)—Cl(2)	156.5(5)	157.042	0.346
N(1)—C(2)—N(2)	106.9(4)	106.695	0.192

[a] Crystallographic data obtained from Garber et al. [10].
[b] Calculated data from this investigation at GCA/PW91/DNP DFT level of theory.

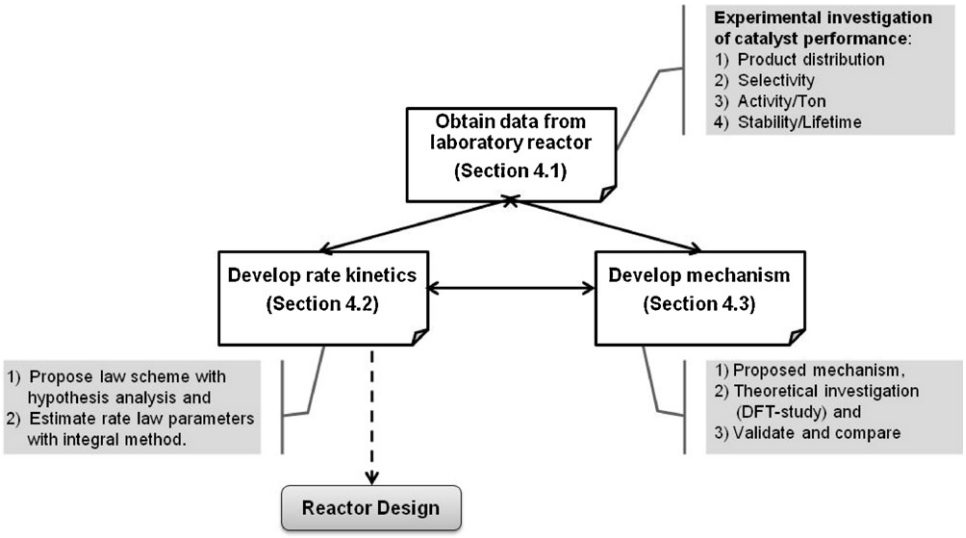

Fig. 2. Methodology framework applied in this study.

Validation of the computational method was based on the structural calculations applied to precatalyst **HGr2**. The geometry of the precatalyst was optimized for the lowest energies and key calculated bond lengths and angles were compared with crystallographic data obtained by Hoveyda and coworkers [10] as depicted in Fig. 1 and Table 1. It is clear from these results that acceptable correlations were obtained between the calculated values of this investigation and the crystallographic data with an average error of 1.37%.

3. Methodology framework

The standard method proposed by Grubbs and co-workers [36] for evaluating metathesis catalysts performances and the algorithm for designing catalytic reactors proposed by Fogler [37] with an integral method for data analysis was used in this study, as summarized in Fig. 2. The metathesis of 1-octene with precatalyst **HGr2** can produce a complex product distribution as given in Table 2 due to alkene isomerization, self- and cross-metathesis reactions [31–34]. It is evident from Table 2 that three major groups of products can be identified, namely: primary metathesis products (PMP), isomerization products (IP) and secondary metathesis products (SMP). PMP refers to the self-metathesis reaction of 1-octene to form 7-tetradecene (C14) and ethene. IP refers to the double bond isomerization reactions of the terminal to internal alkenes (2-C8, 3-C8 and 4-C8). SMP refers to the cascade of products as a result of cross-metathesis and/or self-metathesis of the isomerization products of 1-octene. The reaction system will therefore be described with respect to: product distribution (PMP, IP and SMP), selectivity and activity. Selectivity can be defined as the ability of the precatalyst **HGr2** to preferentially react with 1-octene to produce PMPs and the inability to form IPs and SMPs [34]. The activity of the precatalyst **HGr2** can be described by the effective turnover number (TON) as defined by the ratio of moles PMP formed per moles precatalyst used [38,39].

Table 2
Possible reactions of 1-octene in the presence of precatalyst **HGr2**.

Reaction	Substrate[a]	Products[a]	
Primary metathesis			
Self-metathesis	$C{=}C_7$	$C_7{=}C_7 + C{=}C$	PMP[b]
Isomerization	$C{=}C_7$	$C_2{=}C_6 + C_3{=}C_5 + C_4{=}C_4$	IP[c]
Secondary metathesis			
Cross-metathesis	$C{=}C_7 + C_2{=}C_6$	$C_2{=}C_7 + C{=}C_6 + C{=}C_2 + C_6{=}C_7$	SMP[d]
	$C{=}C_6 + C_2{=}C_5$	$C{=}C_2 + C{=}C_5 + C_2{=}C_6 + C_5{=}C_6$	
	$C{=}C_6 + C_3{=}C_4$	$C{=}C_3 + C{=}C_4 + C_3{=}C_6 + C_4{=}C_6$	
	$C_2{=}C_5 + C_3{=}C_4$	$C_2{=}C_3 + C_2{=}C_4 + C_3{=}C_5 + C_4{=}C_5$	
	etc.	etc.	
Self-metathesis	$C_2{=}C_6$	$C_2{=}C_2 + C_6{=}C_6$	
	$C{=}C_6$	$C{=}C + C_6{=}C_6$	
	$C{=}C_5$	$C{=}C + C_5{=}C_5$	
	$C{=}C_4$	$C{=}C + C_4{=}C_{4P}$	
	etc.	etc.	

[a] Hydrogens are omitted and geometrical isomers not shown for simplicity.
[b] Primary metathesis products (PMP) refer to the self-metathesis products of 1-octene: i.e. $C_7{=}C_7$ and $C{=}C$.
[c] Isomerization products (IP) refer to the double bond isomerization products of 1-octene.
[d] Secondary metathesis products (SMP) refer to all other self- and cross metathesis products.

Table 3
Catalytic performance of **HGr2** towards 1-octene after 420 min at different temperatures and 1-octene/precatalyst molar ratios with no solvent added.

Temperature (°C)	C8/precatalyst molar ratio	C8 (%)	PMP (%)	IP (%)	SMP (%)	TON
30	5000	81.76	17.79	0.24	0.20	890
30	7000	80.16	19.30	0.27	0.28	1351
30	9000	90.69	8.93	0.30	0.08	804
30	10,000	92.04	7.59	0.28	0.09	531
40	7000	71.82	27.38	0.30	0.51	1916
50	5000	20.82	76.94	0.24	2.00	3847
50	7000	30.16	68.60	0.24	1.01	4802
50	9000	28.44	70.26	0.28	1.02	6324
50	10,000	34.40	64.48	0.25	0.87	6448
50	14,000	61.13	38.10	0.27	0.51	5334
60	7000	16.43	72.13	0.84	10.61	5049
70	7000	14.32	69.43	1.46	14.80	4860
80	7000	7.98	70.68	1.40	19.94	4947
90	7000	5.01	55.77	3.18	36.04	3904
100	7000	20.72	19.55	54.20	5.53	1368

The average experimental error of this study was calculated as ±1.1% at the 95% confidence level (assuming normal distribution of C8, PMP, IP and SMP values).

4. Results and discussion

4.1. Metathesis reaction

4.1.1. Influence of reaction temperature

The influence of the reaction temperature on the metathesis performance of precatalyst **HGr2** was investigated by varying the temperature between 30 and 100 °C. The reaction was monitored by GC/FID to determine the product distribution. The results obtained for a 1-octene/precatalyst molar ratio of 7000 with no solvent present are summarized in Table 3 and Fig. 3. It is clear from the results that reaction temperature has a significant effect on the catalytic performance of precatalyst **HGr2**. As the reaction temperature increases to 50 °C, the product formation towards PMP increases (~19% to 68%), while IP and SMP formations are insignificant (less than ~1%). When the temperature increases above 50 °C, IP and SMP formation becomes important with an exponential increase (~11% to 40%). PMP formation stays relatively constant (~70%) between 50 and 90 °C and thereafter decreases to ~19%. The selectivity stays relatively constant (~98%) from 30 to 50 °C,

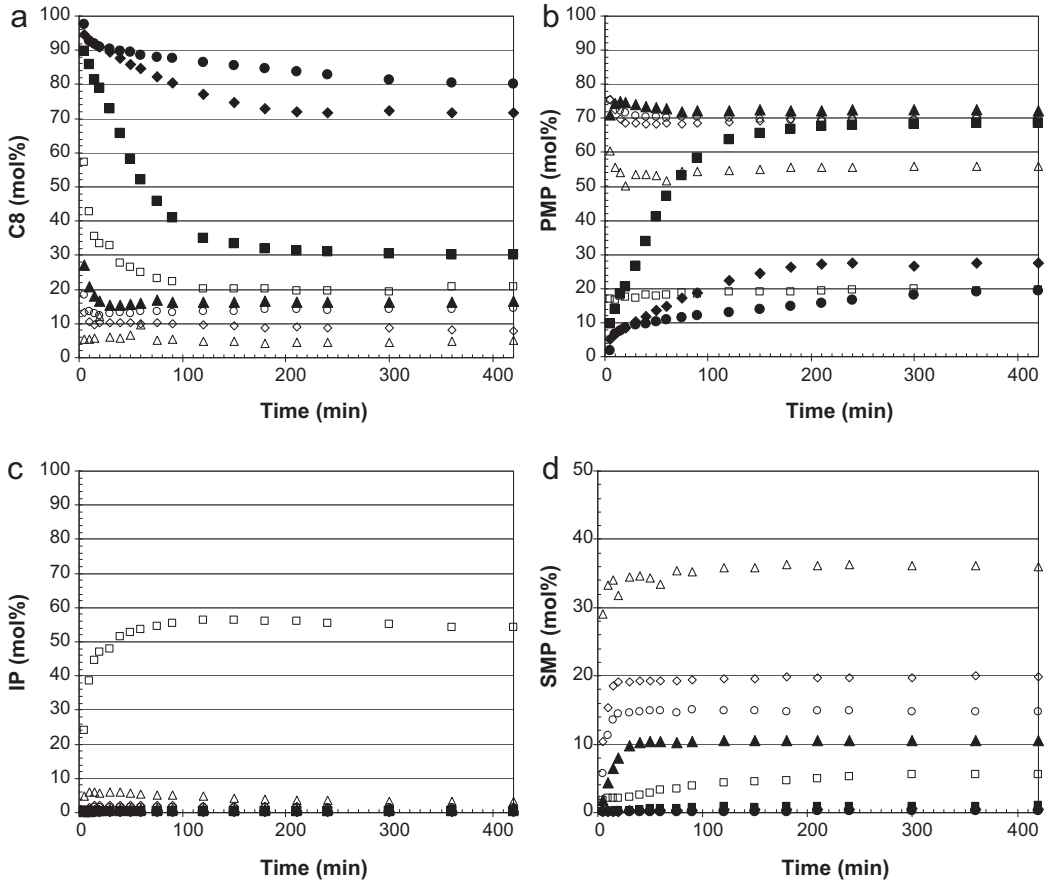

Fig. 3. Typical product distribution profiles at different temperatures: (a) 1-octene consumption, (b) PMP, (c) IP and (d) SMP formations of the 1-octene metathesis reaction with HGr2 at a 1-octene/precatalyst molar ratio of 7000 with no solvent. [(●) 30 °C; (♦) 40 °C; (■) 50 °C; (▲) 60 °C; (○) 70 °C; (◊) 80 °C; (△) 90 °C; (□) 100 °C].

and then decreases (~68% down to ~24%). The turnover number (TON) increases up to 50 °C and then remains relatively constant (~4900) between 50 and 80 °C and decreases thereafter.

From a mechanistic viewpoint, the results indicate that two competing mechanisms are present. The one mechanism is towards the selective formation of PMPs and SMPs (metathesis active mechanism) and the other is selective towards the formation of IP's (isomerization active mechanism). The isomerization active mechanism starts to occur at temperatures above 50 °C, while the metathesis active mechanism is observed for the whole temperature range. Furthermore, it appears from the results that at temperatures above 90 °C, precatalyst **HGr2** starts to lose activity for metathesis and possibly deactivates due to a high reaction temperature environment. Similar results with regard to the formation of IP's with Grubbs-type precatalysts for the self-metathesis of 1-octene were obtained in other studies [40–43]. Lehman et al. [40] for example also found that the isomerization process starts to occur rapidly at temperatures above 60 °C and proposed that the alkene isomerization is promoted by a decomposed catalyst. Forman et al. [35], Dinger and Mol [41] and Hong et al. [42] showed that different Grubbs-type precatalysts can form hydride species that were found to be active and selective alkene double bond isomerization catalysts.

From a reaction engineering point of view, two requirements are extremely important in designing a reactor, i.e. small reactor size and maximization of PMP product. For designing multi-reaction reactors such as this reaction system, the objective must be to minimize the formation of undesired products and to maximize the formation of the desired product, because the greater the amount of undesired product formed, the greater the cost of downstream separation processes. A reactor must therefore be designed in such a way that the selectivity and TON are maximized. From an economic standpoint, maximizing selectivity and TON will maximize profits. The influence of reaction temperature on these two parameters (selectivity and TON) is summarized in Fig. 4. It can be concluded from these results that the desired reaction temperature for designing a reactor for this system must be at low operating temperatures, preferentially 50 °C, as this temperature gave the best relative selectivity and TON.

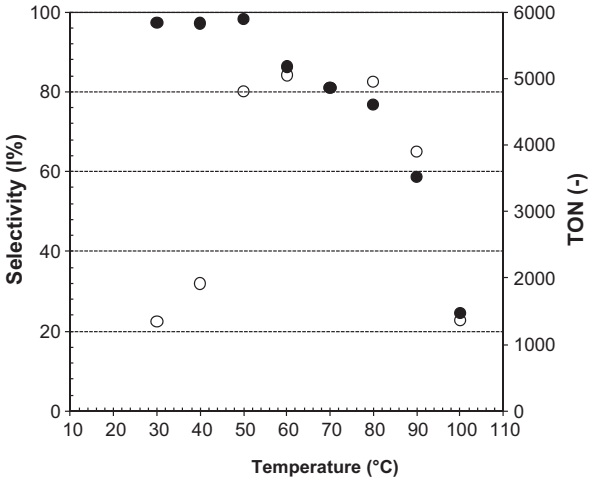

Fig. 4. Influence of reaction temperature on selectivity (●) and TON (○) at 420 min for the 1-octene metathesis reaction with **HGr2** at a 1-octene/precatalyst molar ratio of 7000 with no solvent.

4.1.2. Influence of 1-octene/precatalyst molar ratio

Ruthenium-based metathesis precatalysts, such as **HGr2**, are expensive (timewise and costwise) to prepare and to use from an industrial perspective. It is, therefore, important to investigate the influence of the amount of precatalyst on the metathesis reaction. The temperatures where the **HGr2** precatalyst gave relatively high activity, while retaining a high degree of selectivity and TON with an insignificant amount of IP and SMP products, were found to be below 60 °C (preferentially 50 °C). The influence of 1-octene/precatalyst molar ratio (precatalyst load) was, therefore, further investigated at 30 and 50 °C by varying the 1-octene/precatalyst molar ratio between 5000 and 14,000. The results obtained are presented in Table 3. It is clear from the results that as the 1-octene/precatalyst molar ratio increases (in other words a decrease in precatalyst mass) the product formation towards PMP decreases (~18% to 8% at 30 °C and ~77% to 38% at 50 °C). IP and SMP formation are insignificant because of the chosen operating temperatures. The 1-octene/precatalyst molar ratio did not show any significant effect on selectivity with relatively constant values of ~96% at 30 °C and ~98% at 50 °C. The 1-octene/precatalyst molar ratio, however, did have a significant effect on TON. As the 1-octene/precatalyst molar ratio increases TON also increases to approximately 7000 for 30 °C and 10,000 for 50 °C, where the TON starts to decrease.

4.1.3. Influence of different solvents

In an industrial context, alkene feedstocks derived from primary processes such as the Fischer–Tropsch [44] conversion of synthesis gas often contain numerous impurities that may have the capacity to either retard or completely deactivate various homogeneous catalytic reactions [35]. It is therefore the aim of this section to explore the influence of different organic solvents on the metathesis reaction of 1-octene with **HGr2**. The reactions were carried out at 50 °C with a 1-octene/precatalyst molar ratio of 7000 as these conditions gave relatively high activity, selectivity and TON with insignificant amounts of IPs and SMPs being formed. The molar ratio of 1-octene/solvent was 1. The solvents used to characterize the reaction performance were selected based on their use and presence

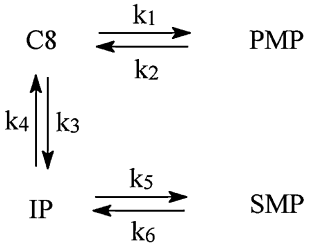

$$\frac{dc_{C_8}}{dt} = -k_1 c_{C_8} - k_3 c_{C_8} + k_2 c_{PMP} + k_4 c_{IP} \quad (1)$$

$$\frac{dc_{PMP}}{dt} = k_1 c_{C_8} - k_2 c_{PMP} \quad (2)$$

$$\frac{dc_{IP}}{dt} = k_3 c_{C_8} - k_4 c_{IP} - k_5 c_{IP} + k_6 c_{SMP} \quad (3)$$

$$\frac{dc_{SMP}}{dt} = k_5 c_{IP} - k_6 c_{SMP} \quad (4)$$

Fig. 5. Proposed reaction scheme and elementary rate equations for the metathesis reaction of 1-octene with precatalyst **HGr2**.

Table 4
Catalytic performance of **HGr2** towards the metathesis of 1-octene after 420 min for different organic solvents at 50 °C.

Solvent	C8 (%)	PMP (%)	IP (%)	SMP (%)	TON
Neat	30.16	68.60	0.24	1.01	4802
Toluene	57.25	41.25	0.52	0.98	2887
Diethyl ether	10.49	69.03	1.97	18.50	4832
Acetic acid	94.53	2.23	3.09	0.15	156
Tetrahydrofuran	96.00	3.16	0.70	0.15	221
Phenol	87.40	11.01	1.50	0.10	771
Ethanol	90.05	2.52	6.73	0.71	177
DMSO[a]	–	–	–	–	–

[a] Dimethyl sulphoxide (DMSO): the reaction showed no metathesis activity with polar and non-polar layer separation.

in typical industrial feed streams. The metathesis results obtained are shown in Table 4. It is clear from the results that the addition of organic solvents had a significant effect on the metathesis, mostly detrimental.

4.2. Empirical reaction kinetic model

According to Dias et al. [13] it appears that Grubbs-based precatalysts can fairly accurately be described by an empirical first-order type of rate equation. The experimental product distribution time curves, for a typical example as shown in Fig. 3, for the metathesis reaction of 1-octene with **HGr2** also depicted a parallel reaction type of scheme. It is, therefore, proposed in this study that the metathesis reaction of 1-octene with precatalyst **HGr2** can be described from a reactor engineering viewpoint by the parallel reaction scheme as postulated in Fig. 5 and the four differential equations as given in Eqs. (1)–(4):

$$\frac{dc_{C8}}{dt} = -k_1 c_{C8} - k_3 c_{C8} + k_2 c_{PMP} + k_4 c_{IP} \quad (1)$$

$$\frac{dc_{PMP}}{dt} = k_1 c_{C_8} - k_2 c_{PMP} \quad (2)$$

$$\frac{dc_{IP}}{dt} = k_3 c_{C8} - k_4 c_{IP} - k_5 c_{IP} + k_6 c_{SMP} \quad (3)$$

$$\frac{dc_{SMP}}{dt} = k_5 c_{IP} - k_6 c_{SMP} \quad (4)$$

The following notation is used in the four rate-law equations:

c_{C_8} concentration of 1-octene in the reactor,
c_{PMP} concentration of PMPs in the reactor,
c_{IP} concentration of IPs in the reactor,
c_{SMP} concentration of SMPs in the reactor,
k_1 forward observed rate constant for the consumption of 1-octene in reaction 1,
k_2 reverse observed rate constant for the formation of 1-octene in reaction 1,
k_3 forward observed rate constant for the consumption of 1-octene in reaction 2,
k_4 reverse observed rate constant for the formation of 1-octene in reaction 2,
k_5 forward observed rate constant for the consumption of IPs in reaction 3 and
k_6 reverse observed rate constant for the formation of IPs in reaction 3.

The value of each observed rate constant (k_1, k_2, k_3, k_4, k_5 and k_6) for the different temperatures and 1-octene/precatalyst molar ratio profiles was determined by regression, using the Simplex method in combination with the Runge–Kutta method to solve Eqs. (1)–(4) simultaneously. The standard error of regression coefficients was determined with the Bootstrap method. The regression results are summarized in Table 5. The observed rate constants of Eqs. (1)–(4) can generally be described by a function of precatalyst concentration and temperature (Arrhenius Equation) as depicted in Eqs. (5):

$$k_{obs} = f(\text{catalyst concentration}) \times g(\text{temperature}) = k \times C_{catalyst}^{\alpha} \times e^{[-E/RT]} \quad (5)$$

where k is the pseudo-frequency or pseudo-pre-exponential factor, $C_{precatalyst}$ is the concentration of the precatalyst used, α is the reaction order that correlates the precatalyst influence, E is the activation energy of the reaction, R is the gas constant and T is the absolute temperature. The observed rate constant parameters

Table 5
Observed rate constants for the reactions of 1-octene with precatalyst **HGr2**.

Temperature (°C)	C8/precatalyst molar ratio	Observed rate constants (min^{-1})
30	5000	$k_1 = 0.0118 \pm 0.0004$, $k_2 = 0.070 \pm 0.002$, $k_3 = 0.0001 \pm 0.0002$ $k_4 = 0.016 \pm 0.009$, $k_5 = 0.0138 \pm 0.0005$, $k_6 = 0.0025 \pm 0.0004$
30	7000	$k_1 = 0.00385 \pm 0.00006$, $k_2 = 0.0198 \pm 0.0003$, $k_3 = 0.00004 \pm 0.00002$ $k_4 = 0.0018 \pm 0.0004$, $k_5 = 0.0012 \pm 0.004$, $k_6 = 0.0015 \pm 0.006$
30	9000	$k_1 = 0.00239 \pm 0.00005$, $k_2 = 0.0271 \pm 0.0006$, $k_3 = 0.00022 \pm 0.00009$ $k_4 = 0.0011 \pm 0.004$, $k_5 = 0.0007 \pm 0.0004$, $k_6 = 0.004 \pm 0.006$
30	10000	$k_1 = 0.00469 \pm 0.00008$, $k_2 = 0.062 \pm 0.001$, $k_3 = 0.00023 \pm 0.00002$ $k_4 = 0.073 \pm 0.003$, $k_5 = 0.0007 \pm 0.0002$, $k_6 = 0.036 \pm 0.004$
40	7000	$k_1 = 0.00403 \pm 0.00002$, $k_2 = 0.01048 \pm 0.00008$, $k_3 = 0.00011 \pm 0.00002$ $k_4 = 0.0077 \pm 0.0002$, $k_5 = 0.0016 \pm 0.0002$, $k_6 = 0.0023 \pm 0.00005$
50	5000	$k_1 = 0.0492 \pm 0.0003$, $k_2 = 0.0149 \pm 0.0001$, $k_3 = 0.0018 \pm 0.0009$ $k_4 = 0.062 \pm 0.008$, $k_5 = 0.030 \pm 0.001$, $k_6 = 0.014 \pm 0.002$
50	7000	$k_1 = 0.01297 \pm 0.00003$, $k_2 = 0.00558 \pm 0.00003$, $k_3 = 0.00038 \pm 0.00009$ $k_4 = 0.031 \pm 0.003$, $k_5 = 0.005 \pm 0.003$, $k_6 = 0.009 \pm 0.004$
50	9000	$k_1 = 0.0312 \pm 0.0001$, $k_2 = 0.0133 \pm 0.0001$, $k_3 = 0.0013 \pm 0.0007$ $k_4 = 0.056 \pm 0.001$, $k_5 = 0.01 \pm 0.01$, $k_6 = 0.02 \pm 0.01$
50	10000	$k_1 = 0.01962 \pm 0.00009$, $k_2 = 0.01044 \pm 0.00008$, $k_3 = 0.00052 \pm 0.0003$ $k_4 = 0.035 \pm 0.005$, $k_5 = 0.0043 \pm 0.0009$, $k_6 = 0.0141 \pm 0.0007$
50	14000	$k_1 = 0.00982 \pm 0.00004$, $k_2 = 0.01526 \pm 0.00007$, $k_3 = 0.0005 \pm 0.0001$ $k_4 = 0.0071 \pm 0.0004$, $k_5 = 0.0019 \pm 0.0007$, $k_6 = 0.0017 \pm 0.0009$
60	7000	$k_1 = 0.347 \pm 0.001$, $k_2 = 0.079 \pm 0.001$, $k_3 = 0.026 \pm 0.003$ $k_4 = 0.413 \pm 0.003$, $k_5 = 1.197 \pm 0.005$, $k_6 = 0.134 \pm 0.006$
70	7000	$k_1 = 0.621 \pm 0.003$, $k_2 = 0.121 \pm 0.001$, $k_3 = 0.123 \pm 0.001$ $k_4 = 0.914 \pm 0.009$, $k_5 = 0.904 \pm 0.007$, $k_6 = 0.112 \pm 0.001$
80	7000	$k_1 = 0.751 \pm 0.001$, $k_2 = 0.106 \pm 0.002$, $k_3 = 0.236 \pm 0.003$ $k_4 = 0.938 \pm 0.006$, $k_5 = 0.945 \pm 0.009$, $k_6 = 0.119 \pm 0.001$
90	7000	$k_1 = 1.629 \pm 0.009$, $k_2 = 0.177 \pm 0.001$, $k_3 = 1.330 \pm 0.001$ $k_4 = 1.519 \pm 0.002$, $k_5 = 0.158 \pm 0.005$, $k_6 = 0.238 \pm 0.007$
100	7000	$k_1 = 2.489 \pm 0.005$, $k_2 = 3.924 \pm 0.007$, $k_3 = 0.0947 \pm 0.0004$ $k_4 = 0.0427 \pm 0.0002$, $k_5 = 0.121 \pm 0.002$, $k_6 = 1.604 \pm 0.001$

Table 6
Calculated constants for the reactions of 1-octene with precatalyst HGr2.

Observed rate constant	Pseudo pre-exponential (k) (min^{-1} $mmol^{-\alpha}$ mL^{α})	Reaction order (α)	Activation energy (E) (kcal mol^{-1})
k_1	3.787×10^{14}	1.39	23.8
k_2	1.245×10^{12}	0.60	15.9
k_3	6.917×10^{24}	1.79	40.9
k_4	1.585×10^{16}	0.56	26.1
k_5	1.172×10^{8}	1.40	30.9
k_6	3.500×10^{12}	0.52	21.4

(k, α and E) as given in Eq. (5) were determined by regression. Statistica© version 10 with the standard nonlinear estimation methods of Levenberg–Marqaurdt and Gauss–Newton was used in the regression process. The regressed values of k, α and E are given in Table 6 and a typical experimental data compared to the kinetic model is presented in Fig. 6. It is evident from these results that the proposed reaction kinetic model of Eqs. (1)–(5) fairly accurately describes the metathesis reaction of 1-octene with **HGr2**.

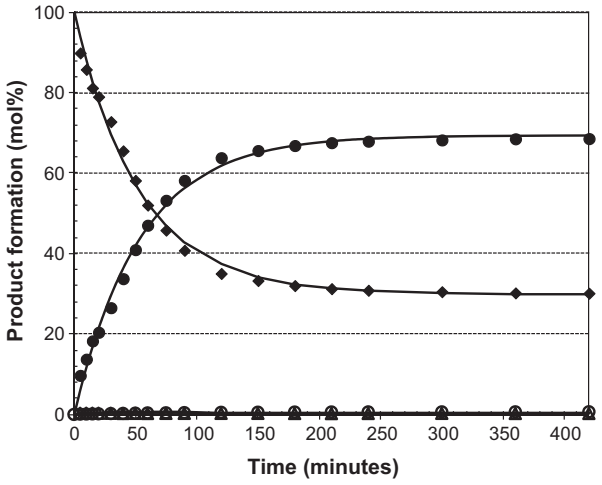

Fig. 6. Experimental data compared to the modelled reaction scheme of Eqs. (1)–(3) for the metathesis reaction of 1-octene with precatalyst **HGr2** at a temperature of 50 °C and 1-octene/precatalyst of 7000 [(●) PMP formation; (△) IP formation; (○) SMP formation; (♦) 1-octene consumption and (—) modelled reaction scheme].

4.3. Mechanism and DFT study

4.3.1. Hoveyda–Grubbs mechanism with 1-octene

Today, the Herisson–Chauvin carbene mechanism is generally accepted as the main alkene metathesis mechanism [45,46]. Furthermore, the dissociative mechanism for the initiation step is well established for the classical phosphine-containing metathesis precatalysts such as Grubbs first- and second-generation. However for the phosphine-free complexes, such as **HGr2**, the initiation mechanism is still debatable at this stage. Three possible initiation mechanisms namely dissociative, associative and interchange have been presented and proved to be feasible for different systems [47–51]. Hoveyda et al. [9] suggested a type of "release-return" mechanism where the initiation step is described by the dissociation of the Ru-O(alkoxy) bond to create a vacant Ru binding site for the incoming alkene substrate. Most of the studies reported focused on this mechanism as it is the simplest and similar to the establish mechanism for Grubbs first and second generation precatalysts. Grubbs and Vougioukalakis [48] suggested an associative mechanism. Recent studies by Vorfalt et al. [47] and Ashworth

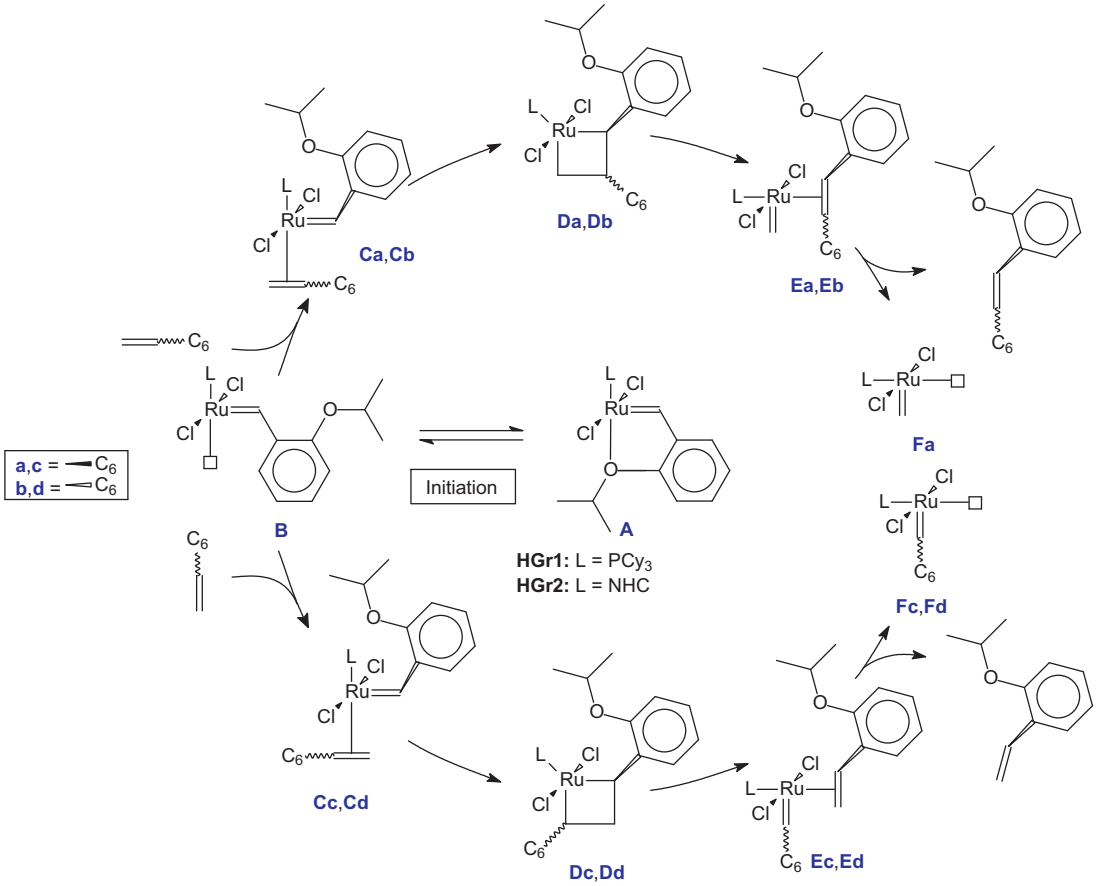

Fig. 7. Initiation and activation steps in the dissociative mechanism for the reaction of 1-octene in the presence of Hoveyda–Grubbs based precatalysts.

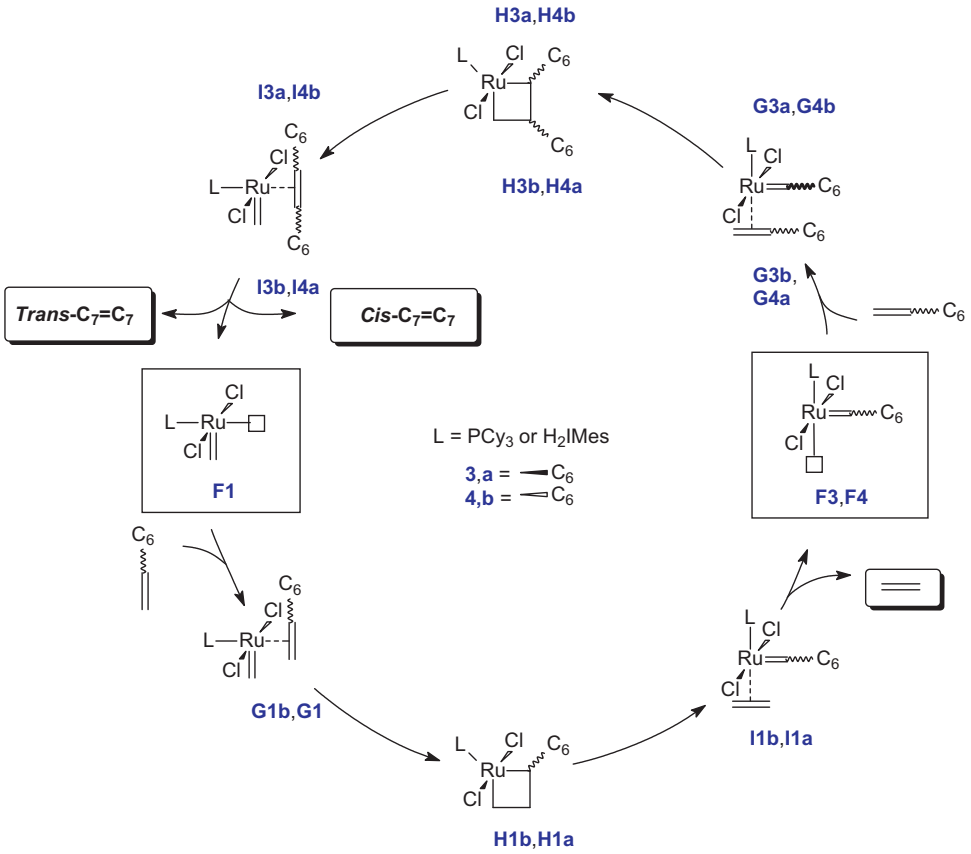

Fig. 8. Catalytic cycle for the productive metathesis of 1-octene with Hoveyda–Grubbs precatalysts.

et al. [49] suggested that the interchange mechanism is possible the more operative mechanism between the three. In this study we decided to use the most simplest and well-known dissociation pathway for the model reaction of 1-octene with **HGr2**. Our approach does not contest the validity of the other mechanism. Conceptually, the productive metathesis of 1-octene in the presence of Hoveyda–Grubbs carbene complexes is depicted in Figs. 7 and 8. The proposed mechanistic model is based upon the general established mechanism suggested by Sanford et al. [14,15,52] and adapted to concepts proposed by Kingsbury et al. [9] and Vorfalt et al. [47] for Hoveyda–Grubbs based precatalysts with the dissociation pathway as initiation step.

The mechanism initializes with the release of the internal oxygen on the 16-electron Ru species **A** to create an open position active 14-electron species **B**. The activation takes place as 1-octene coordinates to the 14-electron intermediate **B** to form the π complex **C**. Complex **C** then undergoes a formal [2+2]-cycloaddition to form a metallacyclobutane ring **D** which in turn returns to a new π complex **E**. The methylidene species **F1** forms with the release of the alkene and then enters the catalytic cycle as illustrated in Fig. 8. When the 1-octene coordinates as shown in **Cc** and **Cd**, heptylidene (**F3**, **F4**) is produced instead of the methylidene complex **F1**. The heptylidene also enters the catalytic cycle. During the catalytic cycle **F1** coordinates with 1-octene to convert either to **F3** or **F4** and produces ethene. Complexes **F3** and/or **F4** coordinates with 1-octene and converts to **F1** to produce either *cis*- or *trans*-7-tetradecene, depending on how the 1-octene coordinates with the heptylidene complex (either into **a** or out **b** of the plane). The cycle will continue to convert methylidene to heptylidene and then the heptylidene back to methylidene to produce ethene and 7-tetradecene until all the 1-octene is converted or, more likely, the precatalyst has dissociated.

4.3.2. DFT investigation of 1-octene metathesis with Hoveyda–Grubbs precatalysts

4.3.2.1. Precatalyst initiation step. It is generally accepted that the Ru-catalysed alkene metathesis reaction with Grubbs first and second generation precatalysts proceeds via a dissociative mechanism, which is initiated by the dissociation of a phosphine ligand from $RuX_2(PR_3)L(=CHR)$ to form a 14-electron species [14,15]. In this sense, the precatalyst's initiation involves the dissociation of the base ligand (PCy_3) from both Grubbs first and second generation. However for Hoveyda–Grubbs based precatalysts the question arises: does the initiation step of dissociation involve the release of the Ru-O-(alkoxy) bond (as depicted in Fig. 9(a)) or rather involve the release of the base PCy_3 or H_2IMes ligands (as depicted in Fig. 9(b)). Summarized electronic energies (ΔE) in kcal mol^{-1} for the different initiation phases ("**A**" to "**B**") with Hoveyda–Grubbs first (**HGr1**) and second (**HGr2**) generation precatalysts are given in Fig. 9. All energies are reported relative to the respective precatalysts "**A**" and balanced with the energies of the free ligand where applicable. It is evident from the results in Fig. 9 that the mechanistic sequence **A** to $\mathbf{B_N}$ is, from an electronic energy point of view, more favourable to occur than the mechanistic sequence **A** to $\mathbf{B_L}$. The reason is that initiation step **A** to $\mathbf{B_N}$ compared to **A** to $\mathbf{B_L}$ gave the lowest electronic energies respectively for both Hoveyda–Grubbs precatalysts. This implies that the release of the Ru—O—(alkoxy) bond to create a vacant Ru binding site would preferentially occur for the metathesis reaction of 1-octene with Hoveyda–Grubbs precatalyst rather than the dissociation step of the base ligand for Grubbs first and second generation precatalysts. The stability effect of the H_2IMes and PCy_3-ligands for the different precatalysts can be compared based on the relative dissociation energies of the ligand, mechanistic sequence **A** to $\mathbf{B_L}$. It is clear from these results that the second generation ligand

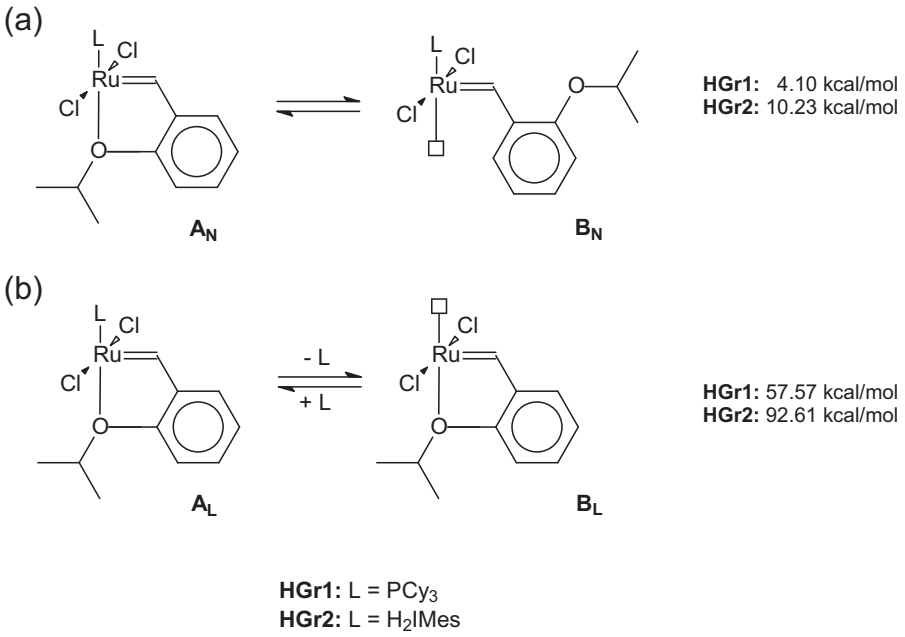

Fig. 9. Initiation step for **HGr1** and **HGr2**. (a) Dissociation of O-atom of the O,C-ligand and (b) dissociation of ligand L.

(**HGr2** = 92.61 kcal mol^{-1}) has a higher dissociation energy than the first generation ligand (**HGr1** = 57.57 kcal mol^{-1}), which means that the H_2IMes-ligand is a more stable ligand than the PCy_3-ligand. Furthermore, the results indicate that the H_2IMes-ligand with its stronger bonding capabilities compared to the PCy_3-ligand, has a significant effect on the initiation step of the forming complex $\mathbf{B_N}$. More energy (thus higher reaction temperatures) is needed for the H_2IMes-ligand based precatalyst than the PCy_3-ligand based precatalyst in the initiation step. This was also found experimentally and with the kinetic study, for example the optimum reaction temperature for **HGr1** is lower (30 °C) then **HGr2** (50 °C). Since it is believed and proven that the hemilabile ligands are to release a free coordination site "on demand" by competing substrates, and occupying it otherwise, the following question arises: does the ruthenium centre of the hemilabile complexes become coordinatively unsaturated with or without the influence of the incoming 1-octene? This implies other mechanistic routes, such as the associative [48] or interchange [47,49] pathways that could lead to different initiation energies. Since ligand initiation via the dissociation mechanism proceeds prior to the interaction of the 1-octene with the ruthenium centre, precatalyst initiation requires the formation of an unsaturated 14-electron complex **B**. Various orientations of the alkylidene moiety in **B** can be possible. According to Janse van Rensburg et al. [53], the alkylidene moiety may be orientated either parallel or perpendicular to the Cl–Ru–X plane (X = Cl or O). They indicated that, for the methylidene species of Grubbs first and second generation precatalysts, different CH_2 orientations could account for the most stable complex, i.e. a parallel orientation of CH_2 for second generation, and perpendicular orientation for first. It was found for this study that the perpendicular orientation gave the lowest geometrically optimized energies for both Hoveyda–Grubbs first and second generation precatalysts.

4.3.2.2. Precatalyst activation step. After the precatalyst initiation step, 1-octene coordinates to the unsaturated intermediate species **B** to form the corresponding π-complexes **C**. Complex **C** then undergoes a formal [2+2]-cycloaddition to form a metallacyclobutane ring **D**, which in turn returns to a new π complex **E** and thereafter the methylidene or heptylidene species (**F**) forms as illustrated in Fig. 8. The coordination of 1-octene with complex **B**, was modelled where 1-octene coordinates in a parallel position to the benzylidene carbene bond (referred to as parallel coordination mode). This mode of coordination was shown to be more energetically favoured for the coordination of alkenes with precatalyst Grubbs first and second generation precatalysts than other modes such as alkene coordination parallel to the Cl–Ru–Cl line and perpendicular or

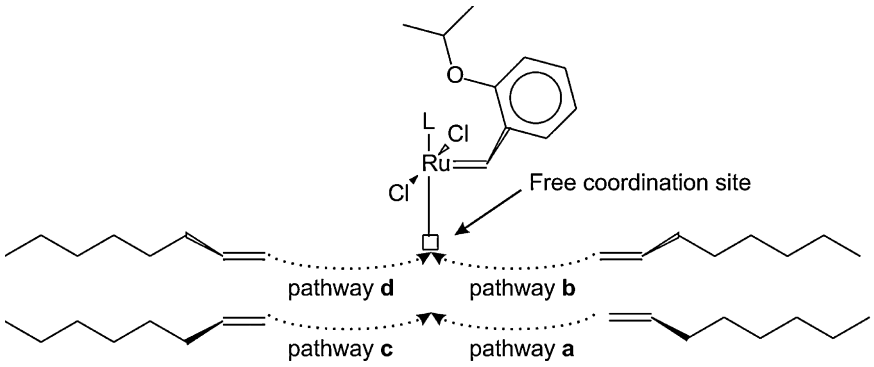

Fig. 10. The four 1-octene coordinating modes, in a parallel position to the benzylidene carbene bond.

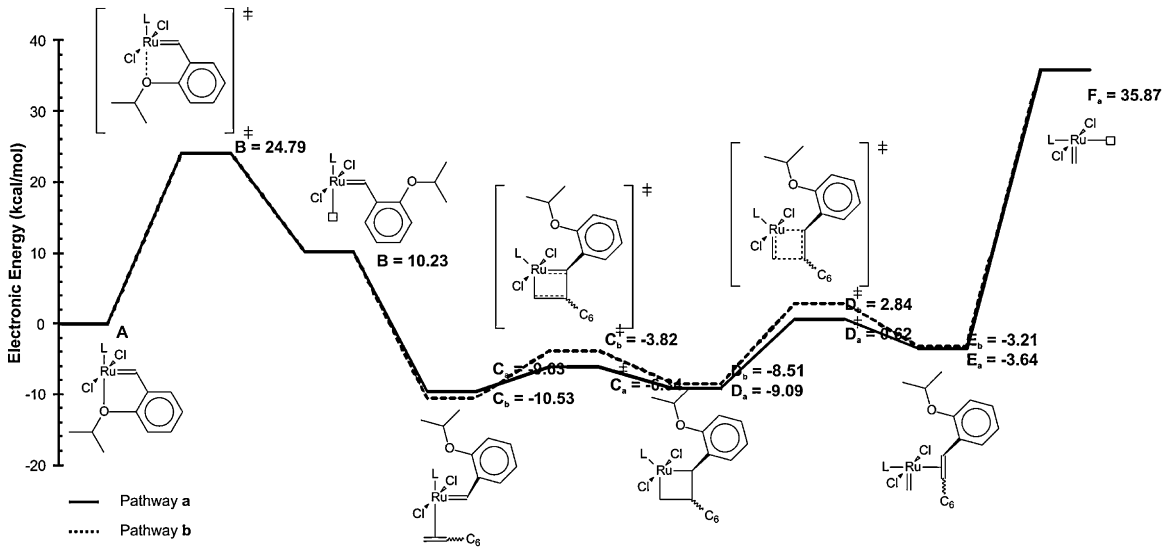

Fig. 11. Electronic energy profiles for the initiation and activation steps of the **HGr2** system for pathways **a** and **b**.

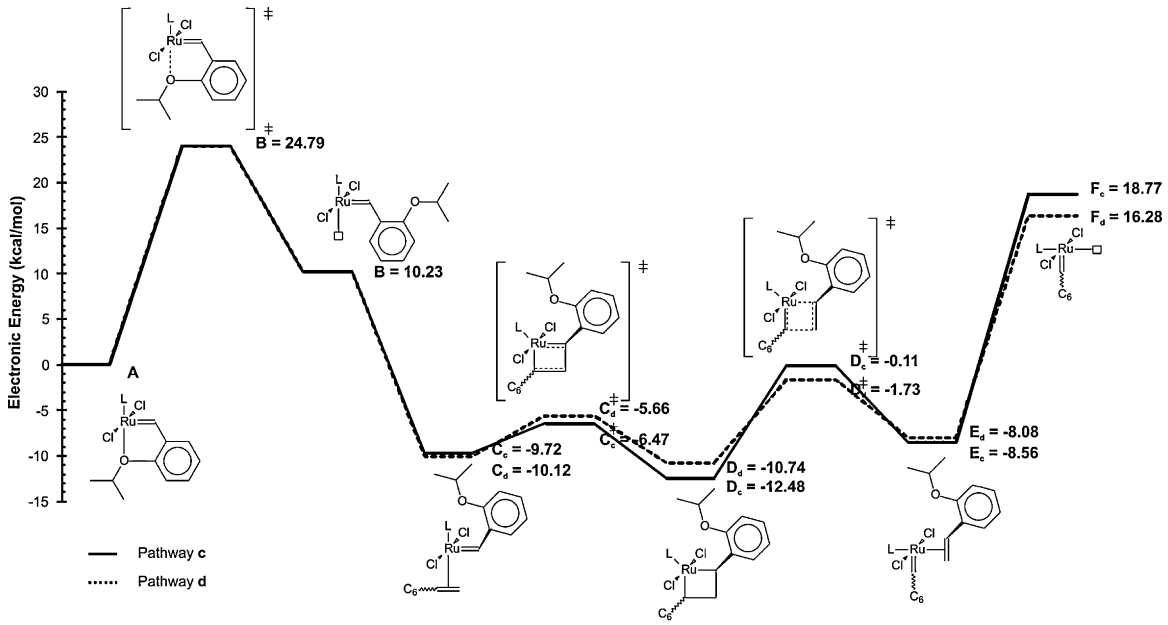

Fig. 12. Electronic energy profiles for the initiation and activation steps of the **HGr2** system for pathways **c** and **d**.

orthogonal to the carbine [53]. Furthermore, the incoming 1-octene can enter the free coordination site of complex **B** in four pathways, as depicted in Fig. 10. The different electronic energy profiles for the initiation and activation steps (complexes **A–F**) for all four pathways are given in Figs. 11 and 12. It is clear from the different pathway results that pathways **c** and **d** are, from an electron energy viewpoint, the most favourable pathways and would preferentially be followed for the generation of 7-tetradecene. The favourable pathways of **c** and **d** are primarily due to the free rotation of the phenyl-based-rings on the alkylidene moiety, which increases the steric bulk around the Ru-centre and, therefore, obstructs coordination of 1-octene to the Ru=C-moiety in pathways **a** and **b**, but to a lesser extent for **c** and **d**. The rate-limiting step for the Hoveyda–Grubbs systems was found to be the initiation step (**A–B**). Furthermore, the theoretically calculated overall initiation energy (24.79 kcal mol^{-1}) correlates well with the experimentally activation energy (23.8 kcal mol^{-1}).

5. Conclusion

In this study, the catalytic performances, reaction engineering kinetics and mechanistic DFT-study of the Hoveyda–Grubbs second generation precatalyst was evaluated for the model reaction of 1-octene to 7-tetradecene. The effect of temperature was significant for product distribution and showed competing mechanisms that are involved, namely metathesis and isomerization. At low temperatures, below 60 °C, the precatalyst showed mainly metathesis activity while at higher temperatures, above 60 °C, it showed both metathesis and isomerization activity. Furthermore, precatalyst **HGr2** demonstrated secondary metathesis products above 60 °C. Precatalyst **HGr2** showed overall detrimental effects when different organic solvents were introduced to the reaction environment. The reaction system was fairly accurately described by the reaction rate-laws as given by Eqs. (1)–(4) with the observed rate constant as a function of precatalyst concentration and temperature. The

mechanistic model and DFT-calculated energy values correlated well with the empirical kinetic model's activation energy and thus validate the two approaches in describing the system.

Acknowledgements

The authors wish to thank the South African Department of Science and Technology - National Research Foundation's Centre of Excellence in Catalysis (c*change) and the North-West University for financial support.

References

[1] C. Samojłowicz, M. Bieniek, K. Grela, Chem. Rev. 109 (2009) 3708.
[2] A.H. Hoveyda, A.R Zhugralin, Nature 450 (2007) 243.
[3] R.H. Grubbs (Ed.), Handbook of Metathesis, vol. 3, Wiley-VCH, 2003.
[4] S.T. Nguyen, L.K. Johnson, R.H. Grubbs, J.W. Ziller, J. Am. Chem. Soc. 114 (1992) 3974.
[5] S.T. Nguyen, R.H. Grubbs, J.W. Ziller, J. Am. Chem. Soc. 115 (1993) 9858.
[6] P. Schwab, M.B. France, J.W. Ziller, R.H. Grubbs, Angew. Chem. Int. Ed. 34 (1995) 2039.
[7] P. Schwab, R.H. Grubbs, J.W. Ziller, J. Am. Chem. Soc. 118 (1996) 100.
[8] A. Michrowska, K. Grela, Pure Appl. Chem. 80 (2008) 31.
[9] J.S. Kingsbury, J.P.A Harrity, P.J. Bonitatebus, A.H. Hoveyda, J. Am. Chem. Soc. 121 (1999) 791.
[10] S.B. Garber, J.S. Kingsbury, B.L. Gray, A.H. Hoveyda, J. Am. Chem. Soc. 122 (2000) 8168.
[11] S. Gessler, S. Randl, S. Blechert, Tetrahedron Lett. 41 (2000) 9973.
[12] A. Michrowska, L. Gulajski, K. Grela, Chem. Commun. (2006) 841.
[13] E.L. Dias, S.T. Nguyen, R.H. Grubbs, J. Am. Chem. Soc. 119 (1997) 3887.
[14] M.S. Sanford, M. Ulman, R.H. Grubbs, J. Am. Chem. Soc. 123 (2001) 749.
[15] M.S. Sanford, J.A. Love, R.H. Grubbs, J. Am. Chem. Soc. 123 (2001) 6543.
[16] J.A. Love, M.S. Sanford, M.W. Day, R.H. Grubbs, J. Am. Chem. Soc. 125 (2003) 10103.
[17] F. Bernardi, A. Bottoni, G.P. Miscione, Organometallics 22 (2003) 940.
[18] C. Adlhart, P. Chen, J. Am. Chem. Soc. 126 (2004) 3496.
[19] S. Booyens, A. Roodt, O.F. Wendt, J. Organomet. Chem. 692 (2007) 5508.
[20] G.C. Vougioukalakis, R.H. Grubbs, Organometallics 26 (2007) 2469.
[21] E.M. Leitao, E.F. van der Eide, P.E. Romero, W.E. Piers, R. McDonald, J. Am. Chem. Soc. 132 (2010) 2784.
[22] C.E. Diesendruck, E. Tzur, A. Ben-Asuly, I. Goldberg, B.F. Straub, N.G. Lemcoff, Inorg. Chem. 48 (2009) 10819.
[23] A. Poater, F. Ragone, A. Correa, A. Szadkowska, M. Barbasiewicz, K. Grela, L. Cavallo, Chem. Eur. J. 16 (2010) 14354.
[24] E. Tzur, A. Szadkowska, A. Ben-Asuly, A. Makal, I. Goldberg, K. Wozniak, K. Grela, N.G Lemcoff, Chem. Eur. J. 16 (2010) 8726.
[25] J.J. Lippstreu, B.F. Straub, J. Am. Chem. Soc. 127 (2005) 7444.
[26] D. Benitez, E.W. Tkatchouk, A. Goddard, Chem. Commun. (2008) 6194.
[27] L. Cavallo, J. Am. Chem. Soc. 124 (2002) 8965.
[28] S.F. Vyboishchikov, M. Buhl, W. Thiel, Chem. Eur. J. 8 (2002) 3962.
[29] S.F. Vyboishchikov, W. Thiel, Chem. Eur. J. 11 (2005) 3921.
[30] H.C.M. Vosloo, A.J. Dickinson, J.A.K. du Plessis, J. Mol. Catal. A: Chem. 115 (1997) 199.
[31] C. van Schalkwyk, A. Spamer, D.J. Moodley, T. Dube, J. Reynhardt, J.M. Botha, H.C.M. Vosloo, Appl. Catal. A: Gen. 255 (2003) 143.
[32] M. Jordaan, P. van Helden, C.G.C.E. van Sittert, H.C.M. Vosloo, J. Mol. Catal. A: Chem. 254 (2006) 145.
[33] M. Jordaan, H.C.M. Vosloo, Adv. Synth. Catal. 349 (2007) 184.
[34] P. van der Gryp, A. Barnard, J.P. Cronje, D. de Vlieger, S. Marx, H.C.M. Vosloo, J. Membr. Sci. 353 (2010) 70.
[35] G.S. Forman, A.E. McConnell, R.P. Tooze, W. Janse van Rensburg, W.H. Meyer, M.M Kirk, C.L. Dwyer, D.W. Serfontein, Organometallics 24 (2005) 4528.
[36] T. Ritter, A. Hejl, A.G. Wenzel, T.W. Funk, R.H. Grubbs, Organometallics 25 (2006) 5740.
[37] H.S. Fogler, Elements of Chemical Reaction Engineering, 3rd ed., Prentice Hall Inter, 1999, p. 967.
[38] M.B. Dinger, J.C. Mol, Adv. Synth. Catal. 344 (2002) 671.
[39] S. Maechling, M. Zaja, S. Blechert, Adv. Synth. Catal. 347 (2005) 1413.
[40] S.E. Lehman, J.E. Schwendeman, P.M. O'Donnell, K.B. Wagener, Inorg. Chim. Acta 345 (2003) 190.
[41] M.B. Dinger, J.C. Mol, Organometallics 22 (2003) 1089.
[42] S.H. Hong, D.P. Sanders, C.W. Lee, R.H. Grubbs, J. Am. Chem. Soc. 127 (2005) 17160.
[43] F.C. Courchay, J.C. Sworen, I. Ghiviriga, K.A. Abboud, K.B Wagener, Organometallics 25 (2006) 6074.
[44] M.E. Dry, In: I.T. Horvath (Ed.), Encyclopedia of Catalysis, vol. 3, Wiley-Interscience, New York, 2003, p. 347.
[45] J.L. Herrisson, Y. Chauvin, Makromol. Chem. 141 (1971) 161.
[46] Y. Chauvin, Angew. Chem. Int. Ed. 45 (2006) 3740.
[47] T. Vorfalt, K. Wannowius, H. Plenio, Angew. Chem. Int. Ed. 49 (2010) 5533.
[48] G.C. Vougioukalakis, R.H. Grubbs, Chem. Eur. J. 14 (2008) 7545.
[49] I.W. Ashworth, I.H. Hillier, D.J. Nelson, J.M. Percy, M.A. Vincent, Chem. Commun. 47 (2011) 5428.
[50] X. Solans-Monfort, R. Pleixats, M. Sodupe, Chem. Eur. J. 16 (2010) 7331.
[51] F. Nunez-Zarur, X. Solans-Monfort, L. Rodriguez-Santiago, R. Pleixats, M. Sodupe, Chem. Eur. J. 17 (2011) 7506.
[52] M.S. Sanford, J.A. Love, in: R.H. Grubbs (Ed.), Handbook of Metathesis, vol. 1, Wiley-VCH, 2003, p. 112.
[53] W. Janse van Rensburg, P.J. Steynberg, M.M. Kirk, W.H. Meyer, G.S. Forman, J. Organomet. Chem. 691 (2006) 5312.